Energetics-Informed Hexapod Gait Transitions Across Terrains

Navinda Kottege[1], Callum Parkinson[1,2], Peyman Moghadam[1], Alberto Elfes[1] and Surya P. N. Singh[3]

***Abstract*— Legged robots offer the potential of locomotion across various types of terrains. Different terrains require different gait patterns to enable greater traversal efficiency. Consequently, as a legged robot transitions from one type of terrain to another, the gait pattern should be adapted so as to maximise traction and energy efficiency. This paper explores the use of power consumption as estimated by the robot in real-time for guiding this gait transition in the case of statically-stable locomotion. While moving, the robot autonomously assesses its power consumption, relates it to the traction, and switches between gaits so as to maximise efficiency. In this way, the robot only needs proprioceptive sensors and consequently does not require velocity estimation, ground imaging or profiling to maintain efficient locomotion across different terrains. The approach has been tested on a hexapod robot traversing a variety of terrain types and stiffness, including concrete, grass, mulch and leaf litter. The experimental results show that gait switching on energetics alone enables traction maintenance and efficient locomotion across different terrains. We also present comparisons between the power consumption metric used in this work and cost of transport which is used in the literature for characterising energetics for legged locomotion.**

I. Introduction

Legged robots provide exceptional locomotion and transport over a larger diversity of environments than similarly sized wheeled or tracked vehicles. By varying locomotion patterns, legged robots can not only adapt to suit varying ground conditions but also can traverse more efficiently [1], [2], [3]. The efficiency of locomotion is often driven by the energy costs of locomotion. From an ecological viewpoint, animals also attempt to minimise the energy costs of their locomotion in order to maximise the energy available for growth and reproduction [4]. While various gait transition mechanism have been proposed for robotics [5], [6] this paper adapts an energetic efficiency focus. Nishii [7], [8] develops an analytical estimate of energy cost for legged locomotion; proposes that the minimisation of the transport cost is a fundamental strategy used by legged animals to define stride period, stride length and other locomotion parameters; and shows how insect gait selection is driven by minimisation of energy cost. One important result of their work is that the author shows quantitatively how lower duty factor gaits such as the alternating tripod gait are more energy efficient at higher locomotion speeds, which accords with studies of insects walking. A limitation of Nishii's work is that it is only limited to a single given terrain and does not address the effect of different terrain types on gait selection and energy cost. We attempt to address this by presenting experimental results and insights on how the energetic cost varies for different gaits on different terrains at different speeds. In this paper, gait transition, or the process of selecting gait patterns across different terrains, is addressed using an energy-based metric in which the power loading drives the selection of gait type.

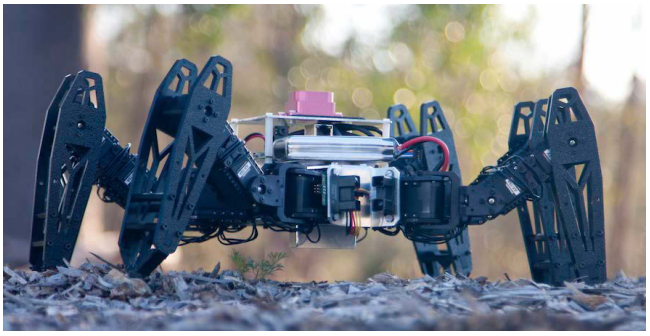

Fig. 1. A modified PhantomX Hexapod robot [15] used to test the adaptive gait transition strategy for efficient locomotion over different terrain types.

In contrast to approaches based on explicit terrain classification for gait adaptation [9], [10] on varying terrain, our method does not require running terrain classifiers, which often require extensive training over a large number of terrain types and may not extrapolate well to new, unseen environment types. Additionally, terrain classifiers often require exterioceptive terrain sensing using vision or LiDAR [11], which add complexity and may only work in certain conditions (e.g., daylight or Lambertian reflectance). Furthermore, terrain that is visually similar may have significantly different mobility characteristics, as traction is primarily force dependent and consequently dependent on the actual ground characteristics [12].

The problem we address, gait transitioning is distinct from dynamic gait adaptation as the former is focused on gait cycle selection where as the latter is focused on optimising locomotion efficiency of a single given gait cycle [4], [7]. This is separate from footfall planning [13] as we assume that all portions of the terrain may accept a foot placement. The strategy of using energetics to inform gait switching is not only analogous to biological systems [14], but has also been used in wheeled robotics [12].

The main contributions of this paper can be summarised as follows: We propose an adaptive gait transition method based on minimising the energy expenditures on locomotion which does not explicitly rely on velocity estimates. We

[1] N. Kottege, P. Moghadam and A. Elfes are with the Autonomous Systems Program, CSIRO, Pullenvale, Brisbane, QLD 4069. Correspondence should be addressed to navinda.kottege@csiro.au

[2]C. Parkinson was with the Autonomous Systems Program, CSIRO at the time this work was carried out.

[3]S. P. N. Singh is with the School of Information Technology and Electrical Engineering, The University of Queensland, Brisbane QLD 4072.

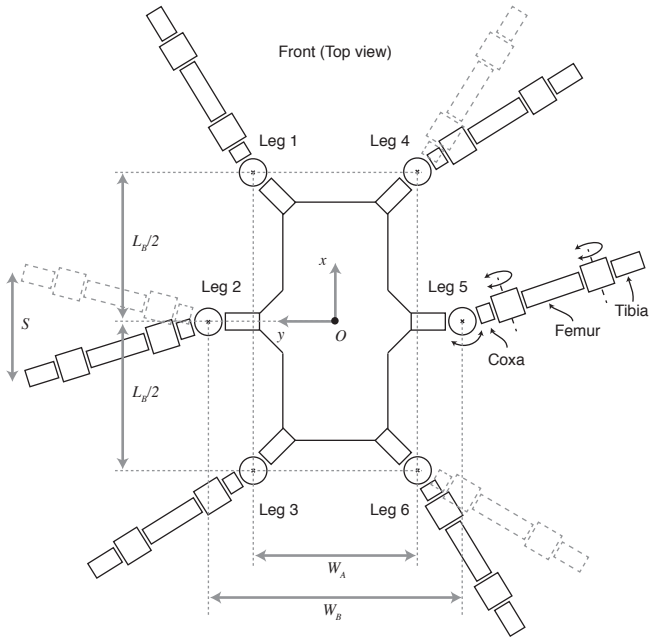

Fig. 2. Hexapod robot model showing legs 1, 5 and 3 in stance phase and legs 2, 4 and 6 in swing phase during an alternating tripod gait. L_B is the body length, W_A and W_B are the lower and upper bounds on the body width, and S is the stride length. The robot's centre of mass is at O, and the positive direction of the x axis corresponds to forward motion.

experimentally evaluate this strategy to show its effectiveness and validate the metric we use against the standard cost of transport. We also present experimental results and insights in to the impact of different gaits, speeds and terrain types on the energy expended during locomotion.

The paper is organised as follows. Section II gives a parametric description of the hexapod platform used in the experiments (shown in Fig. 1) provides a brief overview gait patterns and properties. Section III discusses the power load estimation method and the energetics-informed gait transition algorithm. Section IV describes the experimental setup and procedure and Section V present experimental results showing overall system performance across concrete, grass, and leaf litter. Section VI concludes the paper with insights in to the significant results of this work.

II. Hexapod System

A. Hexapod model

The approach presented in this paper is applicable to legged locomotion in general. However, we will focus on a hexapod robot where each leg has three actuated joints (thus resulting in 18 degrees of freedom (DOFs)). The actuators link the coxa, femur and tibia segments. For clarity of discussion, we consider the operation of the robot in statically stable modes.

The dimensions of the robot (Fig. 2) are given by the body length L_B and the body widths W_A and W_B (lower and upper bounds on the width). The forward direction corresponds to the positive x axis and up corresponds to the positive z axis forming a right handed coordinate frame. The lengths of the femur and the tibia links are given by L_F and L_T, respectively. The stride length is given by S. A typical triangular foot trajectory is shown in Fig. 3, and corresponds to the motion $T_1 \rightarrow T_2 \rightarrow T_3$. Smoother trajectories can be defined by interpolating over a larger number of points (for example, $T_1 \rightarrow T_4 \rightarrow T_2 \rightarrow T_5 \rightarrow T_3$).

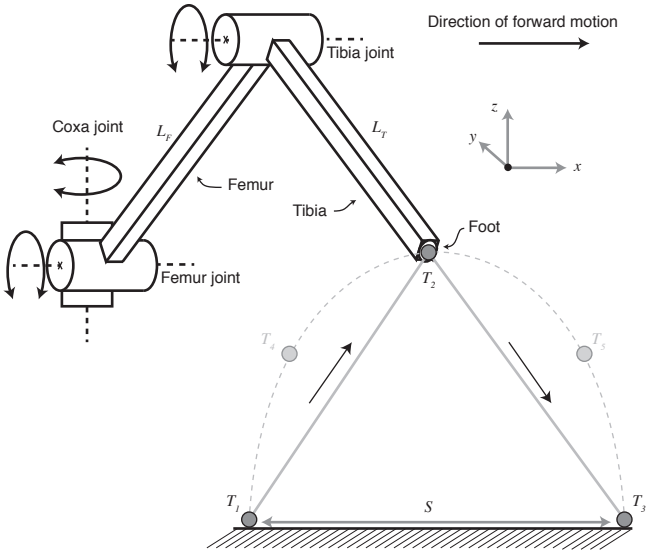

Fig. 3. An example foot trajectory during a stride.

B. Gait patterns

Similar to insects, hexapod robots achieve locomotion by repeatedly executing a "gait pattern". This involves a set of legs pushing back with their feet on the ground thrusting the body forward while the rest of the legs swing forward with their feet off the ground [16]. The legs with feet on the ground are said to be in "stance phase" while the legs swinging forward are in "swing phase". A "stride" for a given leg comprises of a stance phase and a swing phase. Legs repeatedly executing strides result in a gait. The different sequences in which legs can be in stance and swing phase results in different gait patterns. The duty factor β for a leg is defined as

$$\beta = T_{stance}/T_{stride} \tag{1}$$

where T_{stance} is the duration of the stance phase and T_{stride} is the stride period. As noted by Nishii in [7], assuming the

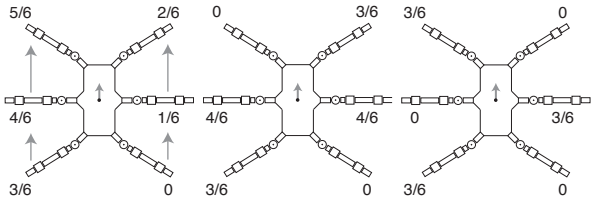

(a) Wave ($\beta = 5/6$) (b) Amble ($\beta = 4/6$) (c) Tripod ($\beta = 3/6$)

Fig. 4. Three standard gait types with the corresponding duty factor $\beta = T_{stance}/T_{stride}$ is the ratio between the duration of the stance phase and the stride period. The numbers alongside the legs denote the relative phase of each leg w.r.t the rear right leg taken as the reference [7].

same duty factor for all legs, $n\beta$ gives the average number of legs in stance phase when n is the total number of legs. Since hexapods require at least three legs on the ground to walk statically, lowest value for β is 0.5.

Typical gaits for an hexapod are wave, diagonal amble and alternating tripod. The duty factors of these gait patterns are given in Fig. 4, while the leg motions during the gait are described next. The leg numbers in examples refer to Fig. 2.

1) Wave gait: The wave gait has one leg in "swing phase" (off the ground) with all other five legs in "stance phase" (on the ground). This pattern is repeated for each leg, leading to a six step gait common among insects. An example wave gait would have the swing phase progress as Leg 3 $\rightarrow$ Leg 2 $\rightarrow$ Leg 1 $\rightarrow$ Leg 6 $\rightarrow$ Leg 5 $\rightarrow$ Leg 4.

2) Amble gait: The diagonal amble gait has two legs in swing phase at a time with four legs in stance phase. This is more common among quadruped animals such as lizards and salamanders. As an example, the swing phase will progress as follows for this three step gait: {Leg 1, Leg 6} $\rightarrow$ {Leg 3, Leg 4} $\rightarrow$ {Leg 2, Leg 5}.

3) Tripod gait: The alternating tripod gait has three legs in stance phase while three are in swing phase. This pattern alternates between the two sets of three legs resulting in a two step gait common among insects when moving fast. As an example, the swing phase progresses as {Leg 1, Leg 5, Leg 3} $\rightarrow$ {Leg 2, Leg 4, Leg 6}.

C. Gait properties

The type of gait and its properties play an essential role in the energy efficiency of the robot. Tripod gaits tend to be fast on hard and level surfaces, but may have higher slippage on loose surfaces, while slower gaits like the amble and wave have higher duty factors (more legs in contact with the ground at any one time) and therefore better traction. To minimise the energy cost of locomotion when traversing different types of terrain, a hexapod robot needs to be able to switch between gaits depending on the properties of the terrain.

The stride frequency, stride length and stride lift height are all properties that affect the performance of a gait. The speed of the hexapod can be increased by increasing the stride frequency and also by increasing the stride length (within workspace limits of the joints). The height the hexapod lifts a leg above ground during a stride also affects the energy consumption. On smooth flat terrain the stride height should be small, as there is no need to step over obstacles. In areas with significant ground cover or small obstacles, the vehicle needs to use a larger stride height to avoid spending more energy to push the legs through obstacles and debris.

In section V we provide an experimental evaluation of how gait properties such as stride frequency can be linked to power consumption and cost of transport across different gaits, terrains and speeds.

III. Energetics and gaits

The energetic cost of transport is a popular metric for characterising energy efficiency for legged robots. Generally, cost of transport[1] is defined the energy required to move a unit mass over a unit distance. Re-adjusting this for power required instead of energy, cost of transport can be written as

$$e = P/mgv \tag{2}$$

where P is the power consumed by the system to cause the motion. In [8] Nishii takes in to account mechanical work done as well as heat energy for legged locomotion and gives cost of transport as

$$e^* = \frac{\sum_{i=1}^{n}(W_i + H_i)}{mgvT_{stride}} \tag{3}$$

where W_i is the mechanical work done while moving leg i, H_i is the heat energy loss for moving leg i, m is the mass of the robot, g is the gravitational acceleration, v is the body speed and T_{stride} is the stride period. Furthermore, the body speed v, under ideal conditions where no leg slips occur due to loss of traction, is related to the duty factor β as

$$v = S/\beta T_{stride} \tag{4}$$

where S is the stride length.

Adapting Eq. 13 from [8] to conform to symbols used in this paper gives mechanical work required to elevate the body accompanied by leg movement in a gait cycle as

$$W_{mech} = \frac{mgS^2}{8nh\beta} \tag{5}$$

where m is the mass of the hexapod in kg, S the stride length in m, h the height of the body above ground in m and n and β being the number of legs and the duty factor. Therefore, by substituting (4) in (5) and dividing by T_{stride}, the mechanical power consumed during motion of the robot is

$$P^*_{mech} = \frac{mgSv}{8nh} \tag{6}$$

These equations establish the relationship between energetic cost of transport, the power consumption and the gait pattern used for legged locomotion.

A. Estimation of Power Consumed

In this paper, we experimentally evaluate how different gait patterns and terrain types affect the power consumption of a six legged robot and present an adaptive gait transition strategy for efficient locomotion over different terrain types. We are interested in doing so without explicit use of body velocity as an input parameter. Compared to the analytical form of mechanical power consumed during locomotion given in (6), we focus on quantities that can be directly measured via proprioceptive sensing at run-time such as the current drawn from the on-board battery. Therefore, the total instantaneous power consumption of the hexapod is estimated as

$$P_{in} = V_{batt} \times I \tag{7}$$

[1]Also referred to as "specific resistance" in the literature

where P_{in} is the instantaneous power consumed by the system in W, V_{batt} is the voltage of the onboard battery in V, and I is the instantaneous current drawn from the battery in A. This total power consumed by the hexapod consists of the power used by the servomotors to generate mechanical power (P_{mech}) and the heat dissipated by the servomotors (P_{heat}). This can be stated as

$$P_{in} = P_{mech} + P_{heat} + \Delta_{loss} \tag{8}$$

where Δ_{loss} represents unaccounted power losses due to factors such as friction.

The amount of mechanical power produced by each motor is related to its rotational speed and torque. The total mechanical power during motion of the system can therefore be given by

$$P_{mech} = \sum_{i=1}^{k} \omega_i \tau_i \tag{9}$$

where P_{mech} is the total mechanical power produced by k servomotors in W, ω_i is the speed of servomotor i in rads^{-1}, and τ_i is the torque produced by servomotor i in Nm. Both the torque and speed of each joint can be read at run-time by querying the servomotors.

In addition to mechanical power the servomotors also produce heat. The amount of heat produced by each servomotor, which relates to the amount of current drawn and the internal resistance of the motor windings. The total power loss due to heat is given by

$$P_{heat} = \sum_{i=1}^{k} I_i^2 R_i \tag{10}$$

where I_i is the current draw of the motor i in A and R_i is the internal resistance of the motor i in Ω. The current drawn by each servomotor will not be equal as the work performed by each joint varies over the gait cycle. However, over a full gait cycle, we assume the average current draw by each of the 18 servos to be the same. Therefore

$$P_{heat} \approx I^2 R \tag{11}$$

Furthermore, to experimentally evaluate the effect of different gaits, speeds and terrains on the cost of transport, we use P_{in} from (7) in (2) to give

$$e_{exp} = P_{in}/mgv \tag{12}$$

Cost of transport plots shown in the following sections use (12) with the velocity measurements obtained via a robotic total station serving as an external ground truth reference.

B. Gait transition

As one of the main contributions of this work, we present an adaptive gait transition method to maintain energy efficient locomotion based on changes in power consumption of the robot. This method was implemented to run in real-time on the robot and we present experimental results showing how this method performs.

The changes in power serves as an indicator of the effectiveness of a gait. By monitoring these characteristics, we can determine when to switch between gaits. This has the advantage of both not requiring a calculation for the speed of the robot and also not requiring specific information about the power consumption of each gait over different terrain. To evaluate this method, two gait types were chosen based on empirical analysis. A fast tripod gait with a short triangular leg trajectory was selected for hard level terrain as it showed the best energy efficiency with lower duty factor ($\beta_{tripod} = 3/6$). A fast wave gait with a long triangular leg trajectory was selected for loose uneven terrain as it has better traction with a higher duty factor ($\beta_{wave} = 5/6$) and the higher leg trajectory is beneficial for clearing obstacles and debris. To switch between the gaits the variation in power consumption was measured and the decision to change gait was done using an adaptive threshold as described in the pseudocode given in Algorithm 1. It is worth mentioning we assume that the robot explicitly does not have any information about the terrain types or its properties.

Algorithm 1 Gait Transition Method

```
function GETGAIT(gait, power, T_elapsed)
    if T_elapsed > T_long then
        if gait = Tripod then
            if |avgPower − power| > P_tripod then
                T_elapsed ← 0
                return wave
        if gait = Wave then
            if |avgPower − power| > P_wave then
                T_elapsed ← 0
                return tripod
    return gait
```

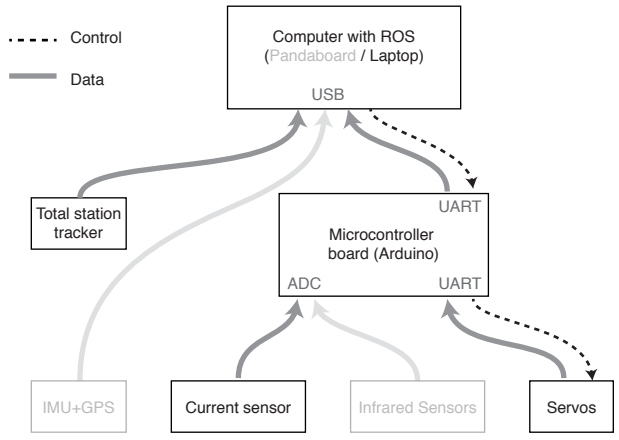

Fig. 5. Hexapod system components showing data and control flows. The components depicted in light grey were not used during the experiments discussed in this paper.

where $gait$ is the current gait type in use by the hexapod, $power$ is the short term average of the instantaneous power P_{in} drawn by the hexapod system, averaged over a

duration of T_{short}, $avgPower$ is the long term average of the instantaneous power drawn by the system P_{in}, averaged over a duration of T_{long}. $T_{elapsed}$ is the duration since the last gait switch which is initialised to be greater than T_{long}. $T_{elapsed}$ is used to enforce a delay of at least T_{long} between gait switches to allow the long term average to re-stabilise. P_{tripod} and P_{wave} are the heuristically estimated power draw tolerances for tripod and wave gaits. When the robot is powered on, the default gait type is set to tripod as empirical results show it is the most energy efficient on flat hard terrain types.

By detecting either an increase in power consumption as the gait encounters resistive terrain or a decrease as traction is lost on slippery ground, the tripod gait can be switched to wave to adapt to the conditions. Furthermore, while executing the wave gait, by detecting drops in power consumption as the terrain becomes more uniform, the gait is switched to a tripod gait taking advantage of the smoother terrain to improve energy efficiency.

IV. Experimental Setup and Procedure

We performed a number of experiments with the hexapod to evaluate the performance of proposed gait transition method as well as the energetic behaviour of the legged robot over different gaits and terrains. The details of the experimental setup are presented next and the experimental procedure described afterward.

A. Hexapod Platform

The experiments were conducted using a modified PhantomX hexapod platform [15]. The PhantomX is an 18 DoF robot with a mass of 2.35 kg. The dimensions of the PhantomX platform with reference to Figs. 2 and 3 are: $L_B = 240$ mm, $W_A = 120$ mm, $W_B = 240$ mm, $L_F = 82$ mm, $L_T = 140$ mm and $L_C = 52$ mm. The height of the body origin above level ground is a configurable parameter and we had it set to a nominal value of $h = 95$ mm for the presented experiments. Each leg has three joints, each driven by a Dynamixel AX-18A servomotor [17] and total of 18 joints for the robot. All the servomotors are connected to an Arbotix robot controller board [18] via a single bus with serial communication and power. They are operated in position control mode by sending a sequence of angular positions to all joints to execute a gait cycle. The gait engine generating pose sequences for different gait types run on the Arbotix board in response to control commands received via serial from a high level controller (A laptop running ROS/Ubuntu in these experiments). Apart from the goal position, many parameters such as joint compliance, torque and angle limits can be set at run-time. The current position, speed, torque[2] and voltage are read from all servos at a rate of approximately 30 Hz. Thermal resistance of each these servomotors was measured to be approximately 4.4 Ω.

The robot is powered by a 3-cell Lithium Polymer battery (11.1 V, 5800 mAh) and a current sensor measures the current draw on this power source. The current sensor is read by the Arbotix board via an A/D channel at a rate of 30 Hz.

The modified PhantomX platform was has additional sensors and processing capabilities which are not used in the presented experiments and are shown in light grey in Fig. 5. For the experiments reported here, a laptop computer running ROS/Ubuntu was interfaced to the robot via a USB-serial tether for data logging and monitoring as well as sending motion commands to the robot during experiments.

B. Ground Truth Position Reference

As a means of establishing accurate external ground truth reference, we use a robotic total station[3] [19] to track the position of the hexapod using a target prism mounted on the robot during experimentation. This system provides x, y, z position of the target with sub-centimetre accuracy and allows us to measure the hexapod's displacement and instantaneous speed over different types of terrain. These measurements are used *a posteriori* to estimate speed of the robot for calculating the cost of transport using (12). The cost of transport is used to show how different gait patterns and terrain types affect the energy efficiency of the robot. Furthermore, we use cost of transport to validate our presented method of power consumption based gait transition which does not use velocity estimates.

C. Gait Energetics Experiments

A number of experiments were conducted using the hexapod platform to better understand how legged locomotion is

[2]The torque directly read from the servos have a maximum update rate of 10 Hz. We overcome this by calculating torque at a higher rate based on angular speed, position error and compliance value.

[3]The Leica TS12 system consists of a tripod mounted pan-tilt head with a laser which automatically tracks a special target prism.

(a) Concrete (b) Grass (c) Mulch (d) Leaf Litter

Fig. 6. Different terrain types on which the experiments were conducted on.

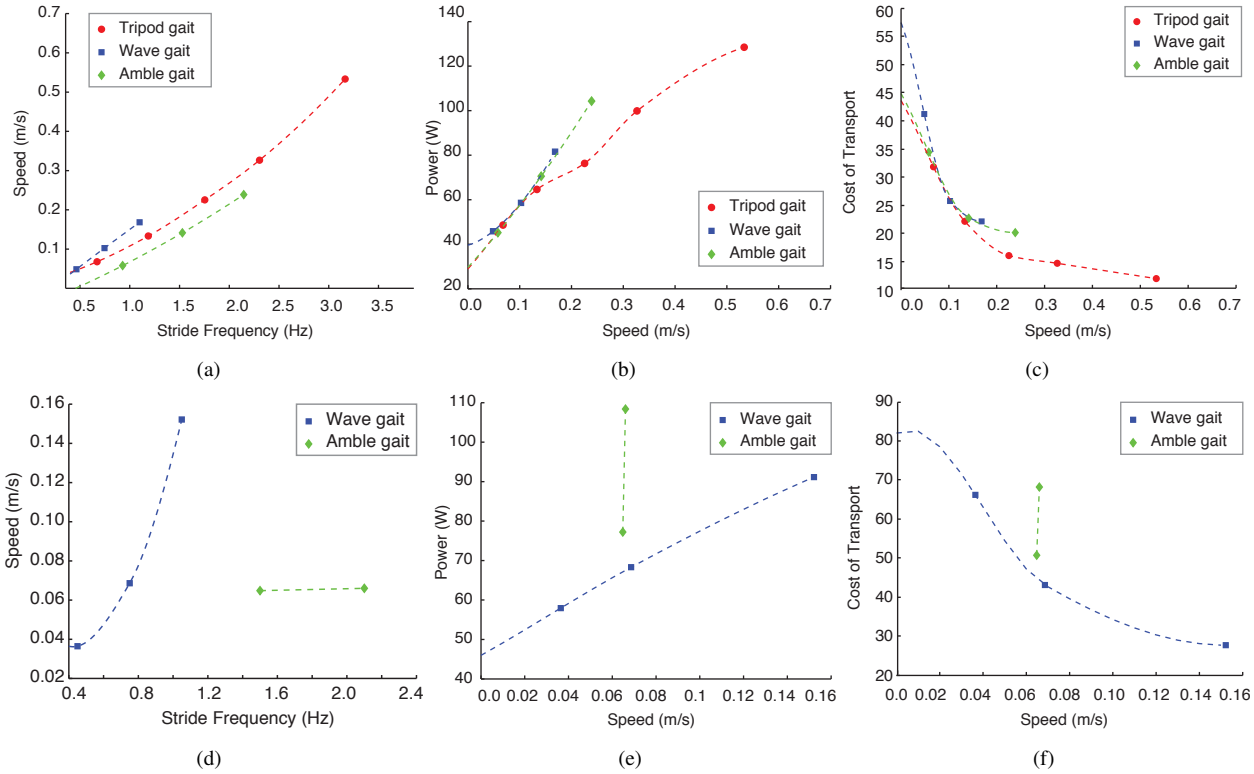

Fig. 7. Forward speed, power consumed and cost of transport for different gaits: (a) - (c) on concrete (a hard, smooth surface); (d) - (f) on leaf litter (a loose uneven surface).

affected by different terrains, gaits and speeds (Fig. 6). The first set of experiments were conducted on a hard smooth concrete surface using three gait types; tripod, wave and amble. These traversals were repeated for different speeds by explicitly changing the stride frequency ($1/T_{stride}$). Each traversal was along a straight line of approximately 16 m in length and was repeated five times and averaged for each stride frequency and gait combination.

A similar set of experiments were then conducted on a natural surface covered with leaf litter representing loose uneven terrain. The fast tripod gait was ineffective in this terrain with the legs of the robot digging in to the surface rather than inducing any forward motion for any of the tested stride frequencies.

D. Gait Transition Experiments

Experiments were conducted to evaluate the performance of our proposed gait transition method by commanding the robot to traverse across terrain boundaries with and without the gait transition algorithm. For one set of experiments, the robot was commanded to traverse from hard smooth concrete surface on to a natural soft surface represented by thick grass with the gait transition algorithm turned off (5× runs). Then the experiments were repeated with the gait transition algorithm turned on. Even with the algorithm turned off, the robot still managed to walk albeit at a slower forward speed since the tripod gait was loosing traction on the soft grass surface. There was a well defined boundary between the two terrain types.

A second set of experiments were conducted by commanding the robot to traverse from a natural uneven surface represented by ground covered by mulch on to a natural loose uneven surface represented by leaf litter with the gait transition algorithm turned on and off. Unlike the previous set of experiments, there was no well defined boundary between the terrain types. It was noticed that the robot got stuck in the leaf litter with hardly any forward motion when gait transitioning was turned off.

The heuristic parameters used for the gait transitioning algorithm discussed in section III-B were set to T_{short}=0.5 s

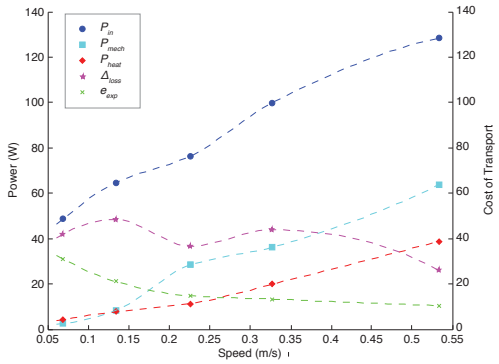

Fig. 8. Total input power P_in (calculated using current draw from battery) compared with mechanical power of the servos P_{mech}, heat dissipated from the servos P_{heat} and other unaccounted power sinks Δ_{loss}. Unit-less cost of transport e_exp is also plotted using (12).

(corresponds to 50 samples), T_{long}=3.0 s (300 samples), P_{tripod}=9.0 W,and P_{wave}=7.2 W. These parameters were selected based on empirical data and set to the same values during all gait transition experiments.

V. Results and Analysis

Here we present the results of the experiments described in the previous section and discuss the significance of our main contributions.

A. Gait Energetics Results

Concrete: The averaged results of experimental runs on the hard concrete surface showing the relationship between stride frequency and forward speed of the robot is given in Fig. 7(a). For each of the runs, the power consumption and cost of transport was calculated using (7) and (12). The power consumption and cost of transport results for these runs are shown in Fig. 7(b) and Fig. 7(c).These tests on concrete show that the tripod gait is the fastest on hard ground. The highest frequency plotted for each gait corresponds to the maximum achievable frequency and consequently maximum speed the hexapod can achieve in that specific gait. The maximum achievable frequency is related to the maximum speed the servos can reach during the swing phase. The shorter the time of the swing phase the quicker the leg must move through it to maintain the proper gait. The duration of the swing phase relates to both the stride frequency $1/T_{stride}$ and duty factor β (Fig. 4), $\beta = 1-(T_{swing}/T_{stride})$. This means that for a given stride frequency the wave gait must move its legs three times as fast during the swing phase compared to the tripod gait and is why the tripod can reach stride frequencies three times that of the wave gait.

Leaf Litter: As mentioned in the experiment description, the tripod gait was ineffective at all tested speeds on this terrain type. Therefore, we only report results for the wave and amble gaits in Fig. 7(d), Fig. 7(e) and Fig. 7(f). These tests on leaf litter show that the wave gait is the fastest on soft, slippery ground. The speed achieved is lower than on concrete as there is loss of traction. The amble gait could only move the hexapod forward when stride frequencies between 1.5 Hz and 2.1 Hz were used. There was no marked improvement in speed with increased stride frequency, as higher frequencies only caused an increase in slippage.

Power consumption: For the set of experiments run on the concrete surface using the tripod gait P_{in}, P_{mech}, P_{heat}, and Δ_{loss} were calculated using equations (7), (9), (11) and (8). These values are plotted against varying speeds in Fig. 8. The unaccounted power loss is significant but shows a drop for higher speeds. The cost of transport e_{exp} is also calculated using (12) and plotted on the same graph for comparison with power consumption for varying speeds.

B. Gait Transition Results

Concrete → grass: Fig. 9(b) shows the hexapod walking from concrete into long grass using a tripod gait. As it moves into the grass a substantial drop in speed can be seen with only a small change in power consumption. Fig. 9(c) shows the hexapod walking across the same terrain boundary, but with our algorithm causing it to switch from tripod to wave gait. While the speed reduction is similar to the previous case, there is a substantial reduction in power consumption,

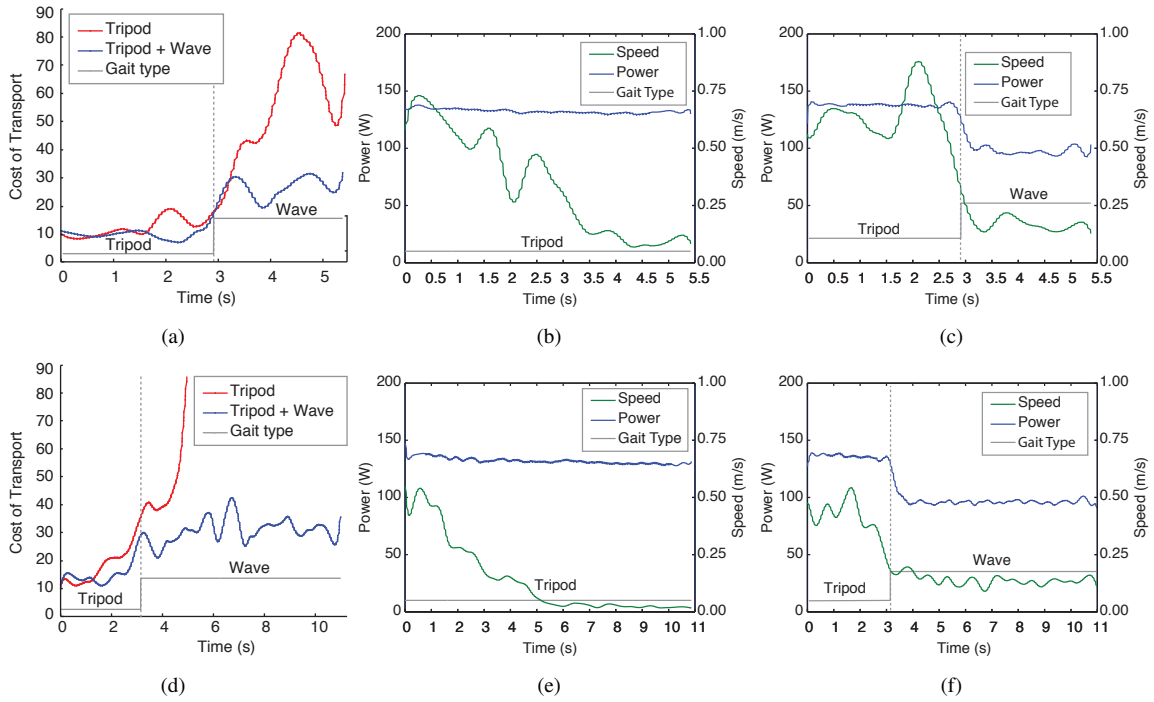

Fig. 9. Energetics performance of gait transition strategy (tripod → wave) compared with using only the tripod gait for concrete → grass transition in (a)-(c) and for mulch → leaf litter transition in (d)-(f). Transition points are depicted by the vertical dashed lines.

since the power consumed by the tripod gait was much higher due to slipping and resistance from the grass. (see also Fig. 9(a))

Mulch → leaf litter: Fig. 9(e) shows the hexapod walking from mulch into leaf litter, again using only a tripod gait. The speed of the hexapod falls to almost zero due to slippage, with again only a small reduction in power consumption. Fig. 9(f) shows the hexapod on the same terrain, transitioning from a tripod to a wave gait, which actually allows it to traverse the leaf litter without getting stuck. Comparing the cost of transport of the two techniques in Fig. 9(d) it can be seen that the tripod gait's cost of transport begins to increase towards infinity as its speed approaches zero whereas the wave gait only increases a finite amount. Overall it can be seen that while there is always an increase in cost of transport when moving from easier to more difficult terrain, the increase can be much smaller by switching gaits as appropriate.

In summary, these results show that even when our proposed method only uses power consumption for transitioning between gaits across different terrains, it allows the hexapod robot to continue with energy efficient locomotion. Furthermore, our proposed method is validated by comparing the power consumption based results with the corresponding cost of transport which is calculated *a posteriori* using the velocity measurement from the total station.

VI. Conclusions

Legged locomotion has long held the promise of enabling robots to traverse far more difficult terrain than can be achieved by wheeled vehicles, but only in recent years has this started to become a reality. One of the major limitations of legged locomotion is its significantly lower efficiency when compared with wheeled locomotion, and hence it is essential to find methods to maximise the efficiency of legged robots. The approach presented in this paper for terrain-adaptive, energetics-informed gait transitions leads to higher efficiency in traversal of multiples types of terrain, and is a step in the right direction. We presented the energy cost of locomotion at different speeds, with different gait types and on various terrains for a six legged robot. Then, we illustrated how power consumption alone can be used for gait transition in run-time allowing the robot not only maintain traction but also to continue with energy efficient locomotion. The power consumption based metric used by our real-time algorithm is compared to the more popular cost of transport metric to demonstrate that our method can trigger gait transitions in a timely manner despite not using a velocity estimate. Given the simplicity and robustness of our method and its reliance on only proprioceptive sensing, it has utility as a fall-back method for more sophisticated gait adaptation methods using exteroceptive sensing.

References

[1] U. Saranli, M. Buehler, and D. E. Koditschek, "RHex: A simple and highly mobile hexapod robot," The International Journal of Robotics Research, vol. 20, no. 7, pp. 616–631, 2001.

[2] J. G. Cham, J. K. Karpick, and M. R. Cutkosky, "Stride Period Adaptation of a Biomimetic Running Hexapod," The International Journal of Robotics Research, vol. 23, no. 2, pp. 141–153, 2004.

[3] M. Hoerger, N. Kottege, T. Bandyopadhyay, A. Elfes, and P. Moghadam, "Real-time stabilisation for hexapod robots," in In proceedings of the International Symposium on Experimental Robotics (ISER 2014), 2014.

[4] D. F. Hoyt and C. R. Taylor, "Gait and the energetics of locomotion in horses." Nature, 1981.

[5] J. G. Nichol, S. P. N. Singh, K. J. Waldron, L. R. Palmer, and D. E. Orin, "System design of a quadrupedal galloping machine," The International Journal of Robotics Research, vol. 23, no. 10-11, pp. 1013–1027, 2004.

[6] H. Pontzer, "Relating ranging ecology, limb length, and locomotor economy in terrestrial animals," Journal of theoretical biology, vol. 296, pp. 6–12, 2012.

[7] J. Nishii, "Legged insects select the optimal locomotor pattern based on the energetic cost," Biological cybernetics, vol. 83, no. 5, pp. 435–442, 2000.

[8] ——, "An analytical estimation of the energy cost for legged locomotion," Journal of Theoretical Biology, vol. 238, no. 3, pp. 636 – 645, 2006.

[9] G. Best, P. Moghadam, N. Kottege, and L. Kleeman, "Terrain classification using a hexapod robot," in Australasian Conference on Robotics and Automation (ACRA '13), 2013.

[10] S. Kajita and K. Tani, "Adaptive gait control of a biped robot based on realtime sensing of the ground profile," Autonomous Robots, vol. 4, no. 3, pp. 297–305, 1997.

[11] M. A. Lewis and L. S. Simo, "Elegant stepping: A model of visually triggered gait adaptation," Connection Science, vol. 11, no. 3-4, pp. 331–344, 1999.

[12] K. Iagnemma and S. Dubowsky, "Traction control of wheeled robotic vehicles in rough terrain with application to planetary rovers," The international Journal of Robotics Research, vol. 23, no. 10-11, pp. 1029–1040, 2004.

[13] K. Hauser, T. Bretl, J.-C. Latombe, and B. Wilcox, "Motion planning for a six-legged lunar robot," in Algorithmic Foundation of Robotics VII. Springer, 2008, pp. 301–316.

[14] A. A. Biewener, Animal Locomotion. Oxford: Oxford University Press, 2003.

[15] Trossen Robotics, "PhantomX AX Hexapod kit [Online]," Available: http://www.trossenrobotics.com/phantomx-ax-hexapod.aspx, accessed: 30-09-2014.

[16] D. M. Wilson, "Insect walking," Annual Review of Entomology, vol. 11, no. 1, pp. 103–122, 1966.

[17] Robotis, "Dynamixel AX-18F e-Manual [Online]," Available: http://support.robotis.com/en/product/dynamixel/ax_series/ax-18f.htm, accessed: 30-09-2014.

[18] Vanadium Labs, "Arbotix Robocontroller [Online]," Available: http://www.vanadiumlabs.com/arbotix.html, accessed: 30-09-2014.

[19] Leica Geosystems, "Viva TS12 [Online]," Available: http://www.leica-geosystems.com/en/Leica-Viva-TS12_91249.htm, accessed: 30-09-2014.